A Review on Multilevel Modular DC/DC Power Converter for High Voltage DC-Connected Wind Energy Applications

Rupali Anil Bodkhe[1], Prof. Parag Jawale[2], Prof. Dr. A.V.Mohod[3]

Student, Dept of Electrical Engineering, PLIT&MS, Buldana (MS), India

Asst. Professor, Dept of Electrical Engineering, PLIT&MS, Buldana (MS), India

Associate Professor, Dept. of Electrical Engineering, PRMCEM, Amravati, (MS), rupali.bodkhe7@gmail.com

Abstract

Recently, the interest in offshore wind farms has been significantly increased because of the stronger and more stable winds at sea, which will lead to a higher power production. DC/DC power conversion solutions are becoming more popular for fulfilling the growing challenges in the high-voltage (HV) dc-connected offshore wind power industry. This paper presents several multilevel modular dc/dc conversion systems based on the capacitor- clamped (CC) module concept for high-power offshore wind energy applications. Two types of the CC modules, namely, the double-switch (DS) module and the switchless (SL) module, are discussed. A soft-switching technique is adopted to achieve minimal switching losses and the maximum system efficiency. Theoretical analysis is carried out for the 2n + 1-level cascaded configurations based on the CC modules. The inherent interleaving property of the proposed configurations effectively reduces the output voltage ripple without adding extra components. A cascaded hybrid topology is developed by the combination of DS and SL modules. The proposed hybrid topology achieves higher efficiency and lower component count. The cascaded hybrid approach is evaluated in terms of the power device count, reliability, and efficiency against other HV dc/dc topologies to demonstrate its advantage for HVDC-connected offshore wind farms. The experimental results of two 5-kW prototype CC converters are presented to validate the theoretical analysis and principles as well as attest the feasibility of the proposed topologies.

Keywords: Capacitor clamped (CC) module, cascaded configuration, double switched (DS) module, offshore wind energy, soft switching technique, switchless (SL) module.

1. Introduction

Offshore wind power must be connected to the onshore power grid for the subsequent distribution and consumption of the generated power. For distant offshore wind power plants, high voltage dc (HVDC) transmission becomes favorable compared to high voltage ac (HV AC) transmission. With the increasing penetration of decentralized offshore wind generation into high voltage power grids, the transmission of electrical energy to the load centers is a major challenge. In this regard, larger wind turbines are leading to increased interest in high power DC/DC converters because of their rigid structure and easy controls [6], [7]. The DC/DC power converters raise the turbine output voltage to the high voltage (HV) level and to provide efficient transmission over long distances [6]-[9]. High voltage transmission using DC technology allows decreases in power losses and cabling cost necessary for large current flow caused by the relatively low voltage of wind turbines. Alternatively, a higher output voltage could be advantageous in order to eliminate a step-up grid coupling transformer which is non-modular, heavy, and bulky [8]-[10]. These bulky and huge electrical components incur high investment and maintenance costs due to more difficult erection,

large cranes, lifting vessels, and equipment transportation from the shore to the installation sites. One of the most important concerns for the converters used in offshore wind farms is their reliability due to the inherent lack of turbine access at sea. Using the modularity, if a single module fails, the converter can still function at a reduced power level. It is also feasible to localize any fault in the system; therefore, the system reliability can be improved. This feature facilitates easier maintenance and obtains a higher mean time between failures. In a modular structure, the total power handling can be allocated equally to multiple modules, allowing the use of cheaper components with low voltage/current stress in the system [11]. Therefore, high power DC/DC conversion systems should be efficient, more compact, and highly reliable due to the more difficult equipment transportation from shore to the installation sites and maintainability of the wind turbines.

In this regard, step-up DC/DC power conversion systems were introduced for future wind farm DC layouts to meet medium voltage (MV) DC and HVDC power requirements. Multiple-module boost converters were represented to achieve a high voltage conversion ratio for offshore wind energy applications connected to an HVDC line [8]. Nevertheless, because of the large duty ratio of the main switch to achieve high voltage gain, the switching frequency is limited to reduce losses and obtain sufficient turn-off time for switches. Therefore, increasing the size of the passive components, such as boost inductors and filter capacitors, is inevitable due to the low switching frequency. In [10] and [12], a step-up resonant (SR) converter was introduced for MVDC levels, in which only one inductor and a single capacitor are used to achieve the high voltage gain and provide a soft-switching technique for the main switches. However, the converter suffers from large power device conduction losses and a high peak-to-peak voltage across the passive components. Moreover, these topologies have a non-modular structure that tends to increase the O&M costs at locations where the marine turbine accessibility is limited. Switched-capacitor (SC) or capacitor-clamped (CC) DC/DC converters have attracted considerable attention in the field of high power applications owing to their high efficiency, high power density, and control simplicity [13]-[17]. In [14] and [15], an SC DC/DC converter with exponential voltage gain for offshore systems was introduced based on the Marx concept. However, large voltage stress of the switches will increase the series connection of power devices, which results in a significant conduction loss and complex balancing circuit. A range of topologies and control methods have been proposed and applied in low power applications. In [11], it was shown that the multilevel modular CC (MMCC) converter featuring fault tolerance has considerable reliability. Soft switching schemes were introduced to reduce switching losses and provide a high efficiency for MMCC topologies. Nevertheless, the voltage stress of capacitors is increased for high voltage gain requirements that results in a low power density. The symmetric MMCC topologies with soft switching schemes were introduced in [17]-[18], which features a high voltage gain with the reduced voltage stress of capacitors and lower switch count, compared to the MMCC topologies in [11]. The output voltage ripple is greatly reduced because of the inherent interleaving property of the symmetric configurations. However, the number of active switches is still large for high power and high voltage applications that the switching devices built to withstand high voltage levels are more expensive. Motivated by these challenges, this paper extends the CC module concept and proposes two different CC module structures, the double-switch (DS) module and active switchless (SL) module. Each module provides a high degree of modularity by the combination of two top and bottom cells. A resonant technique is adopted to achieve a soft-switching scheme for all switches. A combination of SL- and DS-based modules is possible and total power handling is distributed among the components differently to reduce component count and cost for a cascaded hybrid topology. The rest of this paper is organized as follows. In Section II, a detail analysis of the DS- and SL-based modules is presented. Then, 2n+1 level cascaded DS- and SL-based configuration with their properties are demonstrated to achieve a high voltage gain for offshore wind energy

systems. Based on these properties, the cascaded SL-DS- and SIL-DS-based configurations are proposed to reduce component count and cost in the system. Simulation results under steady- and transient-state for a HVDC system are shown in Section III. The experimental results for two 5-kW prototype DS- and SL-based module topologies are presented in Section IV. Finally, the paper is concluded in Section VI. In the MMC, several elementary switching sub-modules are stacked together to attain the required dc operating voltage.

Unlike other high voltage VSC topologies, the MMC avoids the difficulty of connecting semiconductor switches in series. The voltage rating can be scaled by simply adding additional sub-modules to the stack. Thus, it becomes easier to construct VSCs with very high power and voltage ratings. The MMC arrangement also has significantly lower switching losses. A soft switching technique is used to reduce switching losses and provide a high efficiency for MMCC topologies. The capacitor clamped multilevel converter is used for high power offshore wind energy applications. There are two types of the capacitor-clamped modules, the double-switch module and switchless module, are discussed. The cascaded SL- and DS-based topologies are used to achieve the high voltage gains at high efficiency in offshore wind applications. The simulation results are executed by Matlab / Simulink.

2. Proposed modular resonant CC (MRCC) configurations

2.1 Module Structure

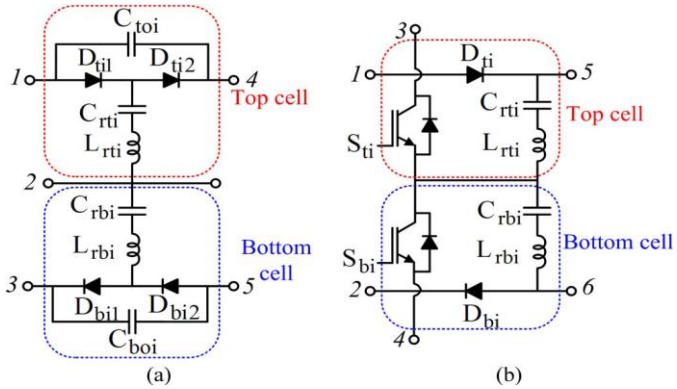

Figure 1. Structure of module (a) SL based module, (b) DS based module

Fig. 1(a) presents an SL-based module, where a five-port system consists of two top and bottom cells. Each cell includes two capacitors, one inductor, and two diodes. The DS-based module is depicted in Fig. 1(b), which is a six-port system with two cells in the top and bottom of the module. Each cell of the DS-based module is composed of a single active switch, one diode, one inductor, and one capacitor. Fig.2 shows the 2*n* + 1-level cascaded configurations of the SL- and DS-based modules. For the cascaded SL-based circuit, an input module is connected to module #1, as shown in Fig. 2(a). For the cascaded DS based topology, ports 5 and 6 of module #*n* are connected to an output module that consists of two capacitors and two diodes [see Fig. 2(b)]. A cascaded SL–DS-based topology will be presented in Section II-E.

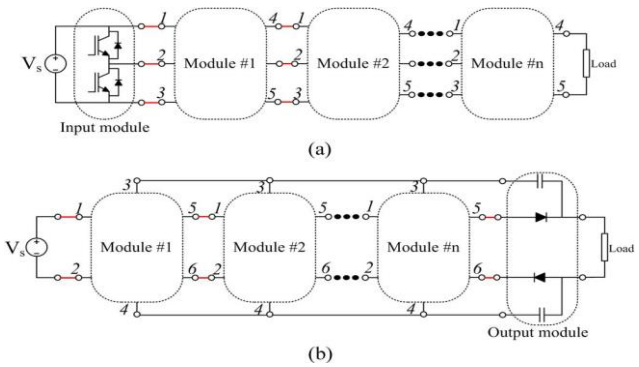

Figure 2. 2*n* + 1-level cascaded configurations. (a) SL-based module. (b) DS-based module.

2.2 Operating Principles of the MRCC Voltage Tripler Converter

To understand the operational principle, the MRCC voltage tripler converter is selected as the topology under analysis. Fig. 3 shows the MRCC voltage tripler converter based on an SL module and a DS module. The MRCC converter consists of an SL-based module indicated by a red-colored box and an input module, as shown in Fig. 3(a). The MRCC voltage tripler can also be realized with a DS-based module represented by a blue-colored box and an output module [see Fig. 3(b)].

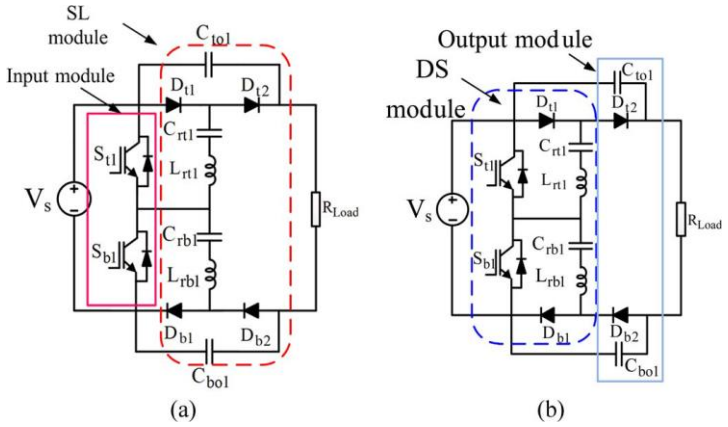

Figure 3. Structure of the MRCC voltage tripler converter (a) SL-based module. (b) DS-based module.

Therefore, both SL- and DS-based configurations have the same circuit for the voltage tripler converter. The active switches S_{b1} and S_{t1} are controlled complementarily with a same duty cycle to minimize the conduction losses for the power devices and passive components. To simplify the analysis, the following assumptions are made.

1) All the switches, diodes, capacitors, and inductors are ideal.
2) The output capacitors C_{to1} and C_{bo1} are large enough to be considered as voltage sources.
3) Two resonant inductors L_{rt1} and L_{rb1} have the same inductances.
4) The resonant capacitors C_{rt1} and C_{rb1} have identical values.
5) V_s is an ideal dc voltage source, and the load is modeled by a pure resistor R_{load}.
6) The switching frequency is less than the resonant frequency to set aside enough dead time for two main switches and achieve a zero-current switching (ZCS). Therefore, the short time interval $[t_1-t_2]$ and $[t_3-t_4]$ are defined as the dead times between active switches to avoid a short circuit in each module.

State I $[t_0-t_1]$ [see Fig. 4(a)]: In the beginning of this mode ($t = t_0$), the bottom switch, S_{b1} is ON; whereas S_{t1} is OFF in the top cell. The charging current flows through D_{t1} and S_{b1}, as shown in Fig.

4(a). Therefore, C_{rt1} is charged by V_s, whereas C_{rb1} is discharged to C_{to1} (C_{rb1} was previously charged at the input voltage level in Mode III) through the resonant loops [see Fig. 5(f)]. The energy of R_{load} is supplied by C_{to1} and C_{rb1}. At $t = t_1$, Sb_1 can be off under the zero-current condition [see Fig. 5(d)].

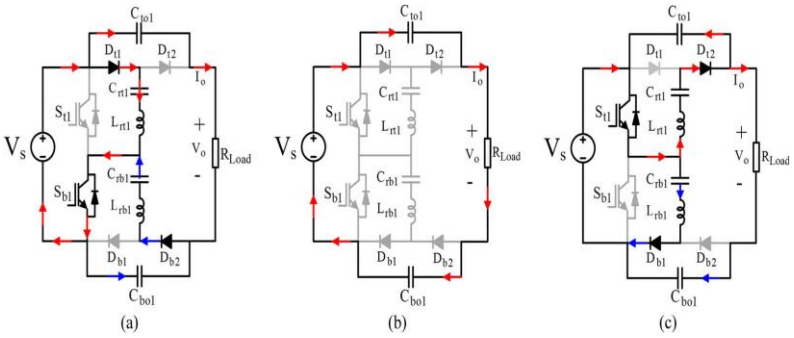

Figure 4. Operating circuits in stages (a) Stage I [t_0–t_1], (b) Stage II [t_1–t_2] and Stage IV [t_3–t_4]. (c) Stage III [t_2–t_3].

State II [t_1–t_2] [see Fig. 5(b)]: In this state, all the switches are turned off. The diodes are reverse biased, and the resonances stop, as shown in Fig. 5(b). Therefore, the inductor currents become zero [see Fig. 6(c)]. The resonant capacitor voltages of C_{rt1} and C_{rb2} are unchanged. C_{to} is connected in series to C_{bo}, and both are discharged to the load terminal.

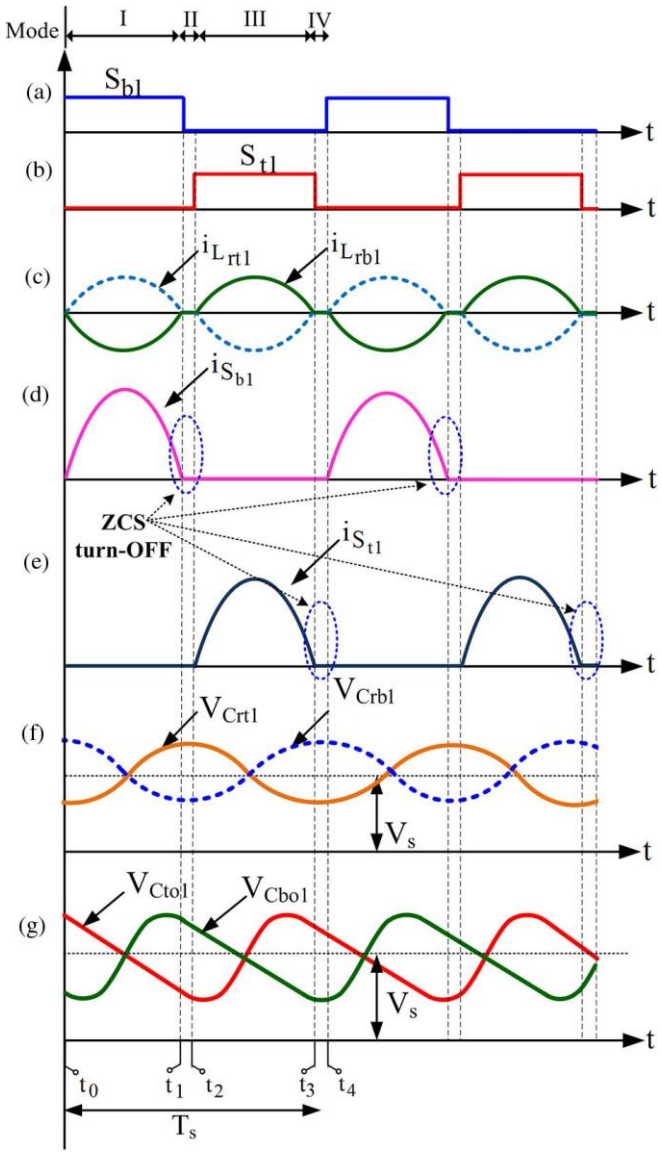

Figure 5. Key current and voltage waveforms of the MRCC voltage tripler converter

State III [t_2–t_3] [see Fig. 5(c)]: After a half-period of the resonant frequency, S_{t1} is turned on, whereas S_{b1} is off. The diodes D_{t1} and D_{b2} are reverse biased by the capacitor voltages. Fig. 6(e) shows that the current through S_{t1}, is increased by a soft-switching operation with a half-cycle resonant shape. In this state, C_{rb1} is charged, whereas C_{rt1} is discharged through two resonant loops, as shown in Fig. 5(c). At time t_3, S_{t1} becomes off under the zero-current condition.

State IV [t_3–t_4] [see Fig. 5(b)]: The operation of this state is similar to that of State II.

2.3 Operating Principles of the 2n + 1-Level Cascaded SL- and DS-Based Configurations

With the same principle, Figs. 6 and 7 show the 2*n* + 1-level cascaded SL- and DS-based topologies, respectively. Note that *n* is an even number in Fig. 7.

Cascaded SL-Based Configuration:

State I [see Fig. 7(a)]: During the period of t_0 to t_1, the bottom switch S_b is on, whereas S_t is off. In each top cell, the diodes D_{ti1}'s (i = 1, 2, . . , n) are forward biased by V_s and C_{toi}'s.

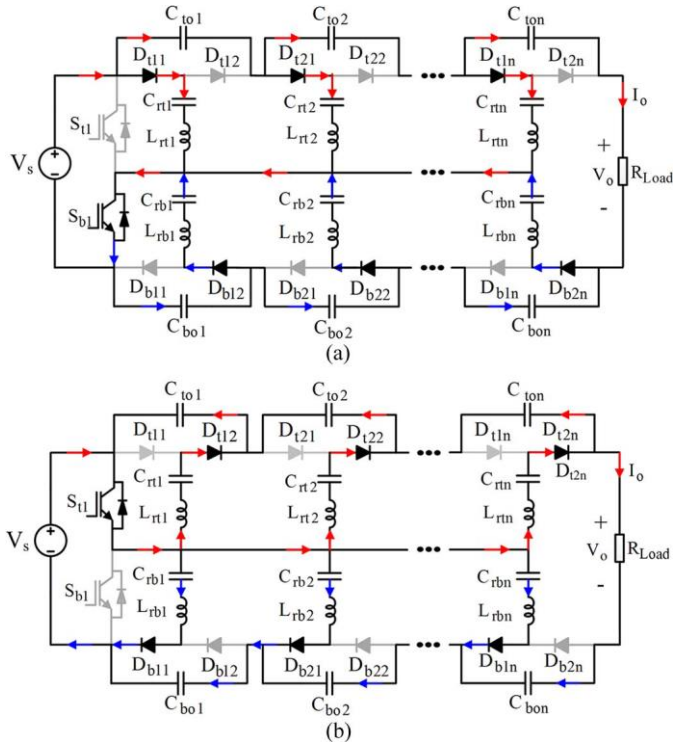

Figure 6. Operation states of the 2*n* + 1-level cascaded SL-based topology. (a) State I. (b) State III.

Therefore, C_{rti}'s are charged by V_s and C_{toi}'s (i = 1, 2, . . . , n − 1), as shown in Fig. 6(a). In this state, C_{ton} is discharged to the load. In contrast, in the bottom cells, C_{rbi}'s are discharged to the output capacitors, C_{boi}'s.

State III [see Fig. 6(b)]: State III begins when the top switch S_t is in the ON-state and S_b is in the OFF-state at t_0. The top diodes D_{ti2}'s and bottom diodes D_{bi1}'s are forward biased, as shown in Fig. 6(b). In the bottom cells, C_{rbi}'s are charged by V_s and C_{boi}'s (i = 1, 2, . . . , n − 1), whereas C_{rti}'s are discharged to C_{toi}'s. As a result, the voltages of C_{rbi}'s are equal to i times the input voltage level.

Cascaded DS-Based Configuration:

State I [see Fig. 7(a)]: At t = t_0, S_{bi} (i = 1, 3, . . . , n −1) and S_{ti} (i = 2, 4, . . . , n) are turned on, whereas S_{bi} (i = even) and S_{ti} (i = odd) are off in the top and bottom cells. Therefore, in the top and bottom cells, the odd numbered C_{rti}'s and even numbered C_{rbi}'s are charged by V_s, C_{rti}'s (i = 2, 4, . . . , n), and C_{rbi}'s (i = 1, 3, . . . , n − 1). In this state, the output capacitor C_{to} is charged by C_{rtn}, whereas C_{bo} is discharged to the load, as shown in Fig. 7 (a).

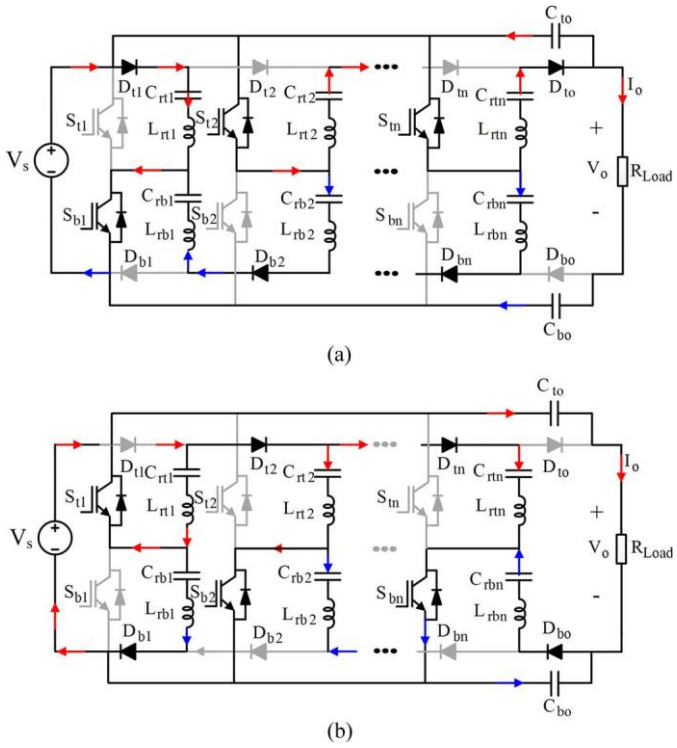

Figure 7. Operation states of the 2*n* + 1-level cascaded DS-based topology. (a) State I. (b) State III. State III [see Fig.8 (b)]: During this time interval, S_{bi}'s (i = 1, 3, . . . , n − 1) and S_{ti}'s (i = 2, 4, . . . , n) are off, here as S_{bi}'s (for i even) and S_{ti}'s (for i odd) are on. Therefore, in the top cells, C_{rti}'s (i = 1, 3, . . . , n − 1) are discharged to C_{rti}'s (i = 2, 4, . . . , n). On the other hand, the odd numbered C_{rbi}'s are charged by V_s and the even numbered C_{rbi}'s.

Table 1. Voltage and Current Ratings of the Components for the SL and DS-Based Configurations

Configuration	SL based	DS based
Voltage rating of resonant capacitor	iV_s (i=1,2,3,…n)	iV_s (i=1,2,3,…n)
Average charging/discharging current rating of resonant capacitor	I_o	I_o
Voltage rating of output capacitor	V_s	nV_s
Average charging/discharging current rating of output capacitor	jI_o (j=n,n-1,…1)	I_o
Voltage rating of switches	V_s	V_s
Voltage rating of diodes	V_s	V_s (i=1,2,3…n) $2V_s$ (i=1,2,3…n-1)
Current rating of switches	$2nI_o$	$2I_o$
Current rating of switches	I_o	I_o

3. Conclusion

HV step-up dc/dc conversion systems are the key-enabling components for offshore wind energy systems to interface with HV transmission networks. In this paper, two CC modules were introduced: the SL- and DS-based modules. A voltage tripler converter based on these modules was analyzed in detail, which minimizes the switching losses significantly. The inherent interleaving property of the proposed modules effectively reduces the output voltage ripple without adding extra components. The cascaded SL- and DS-based topologies were introduced to achieve the high voltage gains at high efficiency in offshore wind applications. These results show that it is possible to develop a cascaded hybrid topology by a combination of the SL- and DS-based modules. Conceptual comparisons of the cascaded hybrid topology with other HV dc/dc approaches show that the proposed converter is well suited for high-power offshore systems that require high efficiency and reliability. The test results have highlighted the performance and feasibility of the proposed topologies.

References

[1] L. Wang and M.S.N. Thin, "Stability analysis of four PSMG based offshore wind farms fed to an SG based power system through LCC-HVDC link ", IEEE Trans. Ind. Electron., vol. 60, no. 6, pp. 2392-2400, June 2013.

[2] T. Kawaguchi, T. Sakazaki, T. Isobe and R. Shimada, "Offshor wind farm configuration using diode rectifier with MERS in current link topology", IEEE Trans. Ind. Electron., vol. 60, no. 7, pp. 2930-2937, Jul 2013.

[3] M.A.Parker, L. Ran and S.J.Finney, "Distributed control of fault tolerant modular multilevel inverter for direct drive wind turbine grid interfacing", IEEE Trans. Ind. Electron., vol. 60, no. 2, pp. 509-522, Feb 2013.

[4] A. Garces and M. Molinas, " A Study of efficiency in a reduced matrix converter for offshore wind farms", IEEE Trans. Ind. Electron., vol. 59, no. 1, pp. 509-522, Jan 2012.

[5] M. Lissere, R. Cardenes, M. Molinas and J. Rodrigueze, "Overview of multi- MW wind turbines and wind parks", IEEE Trans. Ind. Electron., vol. 58, no. 4, pp. 1081-1096, Jan 2011.

[6] A. Parastar and J. K. Seok, "High-power-density power conversion systems for HVDC-connected offshore wind farms," J. Power Electron., vol. 13, no. 5, pp. 746–756, Sep. 2013.

[7] S. P. Engel, N. soltau, H. Stagge, and R. W. De Doncker, "Dynamic and balanced control of three-phase high-power dual-active bridge DC/DC converters in DC-grid applications," IEEE Trans. Power Electron., vol. 28, no. 4, pp. 1880–1889, Apr. 2012.

[8] N. Denniston, A. Massoud, S. Ahmed, and P. Enjeti, "Multiple-module high-gain high-voltageDC–DC transformers for offshorewind energy systems," IEEETrans. Ind. Electron. vol. 58, no. 5, pp. 1877–1886,May2011.

[9] S. Gjerde, P. K. Olsen, K. Ljokelsoy, and T. Undeland, "Control and fault handling in a modular series connected converter for a transformer less 100 kV low weight offshore wind turbine," IEEE Trans. Ind. Appl., vol. 50, no. 2, pp. 1094–1105, Mar./Apr. 2014.

[10] J. Robinson, D. Jovcic, and G. Joos, "Analysis and design of an offshore wind farm using a MV DC grid," IEEE Trans. Power Del., vol. 25, no. 4, pp. 2164–2173, Oct. 2010.

[11] F.H.Khan and L.M.Tolbert, "Multiple-load-source integration in a multilevel modular capacitor-clamped DC–DC converter featuring fault tolerant capability," IEEE Trans. Power Electron., vol. 24, no. 1, pp. 14–24, Jan. 2009.

[12] D. Jovcic, “Step-up DC–DC converter for megawatt size applications,” IET Power Electron., vol. 2, no. 6, pp. 675–685, Nov. 2009.

[13] A. Parastar and J. K. Seok, “High-gain resonant switched-capacitor cell based DC/DC converter for offshore wind energy systems,” IEEE Trans. Power Electron., vol. 30, no. 2, pp. 644–656, Feb. 2015.

[14] E. Veilleux and B. T. Ooi, “Marx-DC–DC converter for connecting offshore wind farms to multiterminal HVDC,” in Proc. IEEE PES, 2013, pp. 1–5.

[15] E. Veilleux, B. T. Ooi, and P.W. Lehn, “Marx DC–DC converter for highpower application,” IET Power Electron., vol. 6, no. 9, pp. 1733–1741, Nov. 2013.

[16] M. L. Gebben et al., “A zero-current-switching multilevel switched capacitor DC–DC converter,” in Proc. IEEE ECCE, 2011, pp. 1291–1295.

[17] D. Cao, X. Yu, X. Lu,W. Qian, and F. Z. Peng, “A double-wing multilevel modular capacitor-clamped DC–DC converter with reduced capacitor voltage stress,” in Proc. IEEE ECCE, 2011, pp. 545–552.

[18] L. He, “A novel quasi-resonant bridge modular switched-capacitor converter with enhanced efficiency and reduced output voltage ripple,” IEEE Trans. Power Electron., vol. 29, no. 4, pp. 1193–1204, Apr. 2014.